Neutron star cooling in various sets of nucleon coupling constants *

DING Wen-Bo(丁文波)[1;1)] YU Zi(喻孜)[2;2)] MI Geng(密更)[3] WANG Chun-Yan(王春艳)[1]

[1] College of Mathematics and Physics, Bohai University, Jinzhou 121000, China
[2] College of Science, Nanjing Forestry University, Nanjing 210037, China
[3] College of Chemistry, Chemical Engineering and Food Safety, Bohai University, Jinzhou 121000, China

Abstract: The influences of nucleon coupling constants on the neutrino scatting and cooling properties of neutron stars are investigated. The results in the GM1, GPS250 and NL-SH parameter sets show that the magnitude of the neutrino emissivity and density ranges where the dUrca process of nucleons is allowed differ obviously between the three parameter sets in nucleon-only and hyperonic matter. Furthermore, the neutron stars in the GPS250 set cool very quickly, whereas those in the NL-SH set cool slowly. The cooling rate of the former can be almost three times more that of the latter. It can be concluded that the stiffer the equation of state, the slower the corresponding neutron stars cool. The hyperon Λ makes neutrino emissivity due to the direct Urca process of nucleons lower compared with nucleon-only matter, and postpones the dUrca process with muons. However, these Λ effects are relatively weaker in the GPS250 set than in the GM1 set.

Key words: nucleon coupling constants, cooling, neutron stars

PACS: 26.60.+c, 21.65.+f, 97.60.Jd **DOI:** 10.1088/1674-1137/37/5/055101

1 Introduction

So far, the matter at the core of compact neutron stars is still poorly known. Many ingredients, such as hyperons [1], antikaon condensations [2, 3], quarks [4] and so on, are all proved to exist reasonably. To limit the equation of state (EoS), there are two main methods. First, the neutron star matter can be probed through observations that measure the mass and radius of stars with high precision. Second, the EoS can be limited by comparing the results of neutron stars from the cooling theory with the observations of thermal radiation. With the accumulation and development of astrophysical observations, research on the second method has attracted much attention. However, it is found that some uncertainties exist in the theoretical study on the cooling properties of neutron stars, and the result differing from various nucleon parameter sets is one factor of the uncertainties. Consequently, a study on how nucleon coupling constants influence the cooling history of neutron stars in theoretical calculations makes good sense.

As we know, in the strong interaction, the properties of neutron star matter, such as meson fields, EoS, the mass and radius of neutron stars et al., are quite sensitive to nucleon coupling constants [1, 5, 6]. Consequently, it is predicted that nucleon coupling constants can also obviously affect the cooling properties of neutron stars. The Fermi momentum of neutrons, protons and leptons in various nucleon coupling constants have been proved to be quite different, which is very crucial to the critical condition of the direct Urca process for nucleons (dUrca process), the most effective cooling mechanism [7–10]. Furthermore, the chemical potentials of leptons, meson potentials, EoS and so on can affect the magnitude of the neutrino emissivity, the neutrino luminosity, and the cooling rate of neutron stars.

By now, several sets of nucleon coupling constants have been obtained and applied to the study of neutron star matter, such as the GM1 set [11], the GPS sets [12], the NL-SH set [13], the TM sets [14] and so on. Although the four bulk properties of nuclear matter at saturation density ρ_0 derived from various nucleon coupling constants are similar, the behavior of the matter at high and superhigh densities is quite different. Accordingly, the input data from the strong interaction to the weak interaction differ violently due to different nucleon coupling constants. In this paper, to investigate the discrepancy of neutron star cooling in various parameter sets, we choose three representative sets of nucleon coupling constants: the GM1 set, the GPS250 set, which leads to very soft EoS, and the NL-SH set corresponding to relatively stiff EoS.

Received 6 June 2012

∗ Supported by National Natural Science Foundation of China (11271055, 11147104)

1) E-mail: dingwenbo1980@gmail.com

2) E-mail: ziyu_njfu@163.com

The cooling properties of stable neutron stars in nucleon-only neutron star matter and hyperonic matter for various nucleon coupling constants will be discussed in the paper at the neutrino emitting stage. The results from the strong interaction, such as the EoSs, the chemical potentials of the leptons, the Fermi momentum of baryons and so on are derived from the relativistic mean field theory (RMFT) in zero temperature approximation. The cooling properties are obtained through the weak interaction theory [7, 15–16]. Note that we only pay attention to neutrinos emitting from the cores of neutron stars, and the radiation in the heat blanketing envelope is neglected.

2 Relativistic mean field and cooling theories

RMFT can successfully describe neutron star matter. Mesons σ, ω and ρ are used to describe the interactions of baryons, and the Lagrangian density is expressed as

$$\begin{aligned} L_{\rm B}=&\sum_{\rm B}\overline{\Psi}_{\rm B}({\rm i}\gamma_\mu\partial^\mu-m_{\rm B}+g_{\sigma{\rm B}}\sigma-g_{\omega B}\gamma_\mu\omega^\mu\\ &-\frac{1}{2}g_{\rho{\rm B}}\gamma_\mu\boldsymbol{\tau}_{\rm B}.\boldsymbol{\rho}^\mu)\Psi_{\rm B}+\frac{1}{2}\partial_\mu\sigma\partial^\mu\sigma-\frac{1}{2}{m_\sigma}^2\sigma^2\\ &-U(\sigma)-\frac{1}{4}\omega_{\mu\nu}\omega^{\mu\nu}+\frac{1}{2}{m_\omega}^2\omega_\mu\omega^\mu-\frac{1}{4}\boldsymbol{\rho}_{\mu\nu}.\boldsymbol{\rho}^{\mu\nu}\\ &+\frac{1}{2}{m_\rho}^2\boldsymbol{\rho}_\mu.\boldsymbol{\rho}^\mu, \end{aligned} \tag{1}$$

where B only denotes nucleons N and hyperon Λ here. $\Psi_{\rm B}$ represents the Dirac spinor for baryon B with vacuum mass $m_{\rm B}$ and $\tau_{\rm B}$ is the isospin operator. $g_{\sigma{\rm B}}$, $g_{\omega{\rm B}}$ and $g_{\rho{\rm B}}$ denote the coupling constants of the σ, ω and ρ meson field, respectively. The scalar self-interaction term [17] in GM1 and GPS250 sets is the same, i.e.,

$$U(\sigma)=\frac{1}{3}bm_{\rm N}(g_{\sigma{\rm N}}\sigma)^3+\frac{1}{4}c(g_{\sigma{\rm N}}\sigma)^4, \tag{2}$$

whereas the one in the NL-SH set reads

$$U(\sigma)=\frac{1}{3}b\sigma^3+\frac{1}{4}c\sigma^4. \tag{3}$$

Through Lagrangian density, the three meson field equations can be obtained. As an object, the conserved baryon number and charge neutrality must be fulfilled in neutron stars,

$$\begin{aligned} \sum_{\rm B}q_{\rm B}\rho_{\rm B}-\rho_{\rm e}-\rho_\mu-\rho_{\rm K^-}=0,\\ \sum_{\rm B}\rho_{\rm B}=n_{\rm B}. \end{aligned} \tag{4}$$

Solving the above nonlinear equations, we can get the Fermi momenta of baryons and leptons, the meson potentials, the chemical potential of leptons, and so on. Consequently, the EoS can be obtained (see Ref. [18] for details). The masses and radii of neutron stars can be derived from the Tolman-Oppenheimer-Volkoff (TOV) equations.

As we know, the most effective cooling mechanism is the direct Urca process of nucleons (the dUrca process), i.e.,

$$\rm n\longleftrightarrow p+e+\overline{\nu}_e, \tag{5}$$

where p, n, e and $\nu_{\rm e}$ denote protons, neutrons, electrons and electronic neutrinos. The neutrino emissivity in one cycle[1,11] can be expressed as

$$\begin{aligned} I_{\rm dUrca}=&\frac{457\pi}{10080}{G_{\rm F}}^2(1+3{g_{\rm A}}^2)\cos^2\theta_{\rm C}T^6{m_{\rm p}}^*{m_{\rm n}}^*\mu_{\rm e}\cdot\\ &\Theta(p_{\rm F_p}+p_{\rm F_e}-p_{\rm F_n}), \end{aligned} \tag{6}$$

where $G_{\rm F}$, $g_{\rm A}$, $\theta_{\rm C}$ are constants in weak interaction, and T represents the interior temperature. $p_{\rm F_i}$ denotes the Fermi momentum, and $m_{\rm n}^*$ and $m_{\rm p}^*$ represent the effective mass of neutrons and protons at the Fermi surface. According to the Landau Fermi-liquid theory, it is known that ${m_{\rm i}}^*=k_{\rm F_i}/v_{\rm i}$. And $v_{\rm i}=({\rm d}\varepsilon_{\rm i}/{\rm d}k)|_{k=k_{\rm F_i}}$ is the Fermi velocity, where $\varepsilon_{\rm i}$ denotes the energy eigenvalue. For neutrons and protons, through RMFT, the effective mass can be expressed as

$$m_{\rm i}^*=\sqrt{k_{\rm F_i}^2+(m_{\rm i}-g_{\sigma{\rm i}}\sigma)^2}. \tag{7}$$

In fact, the Θ function in Eq. (6) corresponds to conservations of energy and momentum, indicating the critical condition of the dUrca process, i.e.,

$$p_{\rm F_p}+p_{\rm F_l}\geqslant p_{\rm F_n}. \tag{8}$$

The chemical potential of electrons $\mu_{\rm e}$, the Fermi momenta of nucleons or leptons $p_{\rm F_i}$ and the effective mass of the nucleon $m_{\rm i}^*$ in Eq. (6) can be obtained from the RMFT. Accordingly these data are quite crucial for neutrino emission. The situation for muons is similar to that for electrons, but the dUrca process for muons starts at a higher density than that for electrons because of the massive mass of muons. The cooling rate of the neutron star can be calculated by the cooling equation

$$C_{\rm v}\frac{{\rm d}T}{{\rm d}t}=-(L_\nu+L_{\rm r}), \tag{9}$$

where $C_{\rm v}$ is the specific heat of the neutron star. L_ν and $L_{\rm r}$ denote the neutrino luminosity and the photon luminosity, respectively.

3 Nucleon coupling constants

Here we exploit the GM1, GPS250 and NL-SH parameter sets for meson-nucleon couplings. The bulk properties of nuclear matter at saturation density for the three parameter sets are shown in Table 1. It is proved

Table 1. The bulk properties of nuclear matter at saturation density for the GM1, GPS250 and NL-SH parameter sets: saturation density ρ_0, binding energy per nucleon B/A, symmetry energy $a_{\rm sym}$, compression modulus K, and Dirac effective mass of nucleons $m^*_{\rm D}/m$. Additionally, the maximum mass $M_{\rm max}/M_\odot$ ($M_\odot$ represents solar mass), the corresponding central densities $u_{\rm cent}$ and radii R of neutron stars in nucleon-only matter for the three parameter sets are shown. u=$n_{\rm B}/\rho_0$, where $n_{\rm B}$ denotes the total baryon number density.

	ρ_0/fm^{-3}	(B/A)/MeV	$a_{\rm sym}$/MeV	K/MeV	$m^*_{\rm D}/m$	$M_{\rm max}/M_\odot$	R/km	$u_{\rm cent}$
GM1	0.153	−16.3	32.5	300	0.7	2.359	11.897	5.65
GPS250	0.153	−16	32.5	250	0.83	1.979	10.970	7.09
NL-SH	0.146	−16.3	36.1	355	0.6	2.797	13.462	4.46

that the EoS in the NL-SH set is the stiffest, whereas that in the GPS250 set is the softest, which is also indicated in the compression modulus. Consequently, the maximum mass of neutron stars in the nucleon-only matter (np matter) in GPS250 is the lowest, but the corresponding central density is the highest, as shown in Table 1. In the paper, we also consider the effect of hyperon Λ. For that, Λ can appear at the lowest density among all the hyperons and it can play a role in neutron star cooling. Experiments show that the Σ hyperon may experience repulsive potentials at high densities. The Ξ hyperon can only appear at super high densities because of the massive mass. So we neglect the effect of the Σ and Ξ hyperons. Here we presume the meson-Λ coupling constant is 0.86 times the meson-nucleon coupling constant to investigate the effect of Λ on neutron star cooling. Neutron star matter with neutrons, protons, leptons and Λ is called "npΛ" matter in the paper.

4 Results

In RMFT, the interactions of baryons are exchanged by mesons, and we show the potentials of mesons in the GM1, GPS250 and NL-SH parameter sets in Fig. 1. It

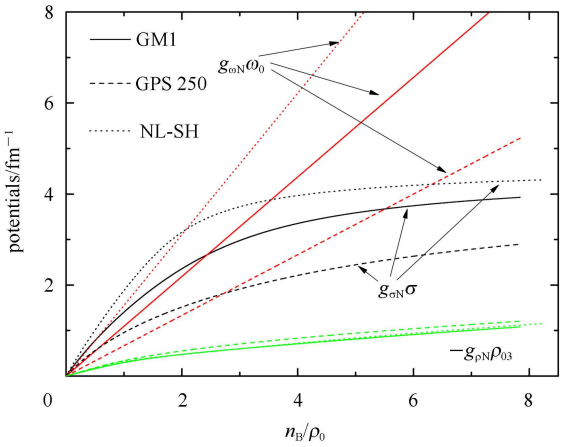

Fig. 1. The mean meson potentials of the σ, ω and ρ meson fields as a function of density in nucleon-only matter in the GM1, GPS250 and NL-SH parameter sets, respectively.

is found that in the σ field, the potential in the NL-SH set (the dotted line) is the highest, whereas that in the GPS250 set (the dashed line) is the the lowest, with the GM1 set (the solid line) being in the middle. According to Eq. (7), it is found that a stronger σ field favors the decrease in the effective mass of nucleons $m^*_{\rm i}$. However, the magnitude of $m^*_{\rm i}$ is also determined by the Fermi momentum $k_{\rm F_i}$, and prevenient results have shown that $k_{\rm F_i}$ increases with the density. The situation in the ω field is similar to that in the σ field. However, in the ρ field, the curve that corresponds to the GPS250 set is somewhat higher than the other two curves, which means that the GM1 and NL-SH sets favor the formation of an isospin saturated symmetric matter.

According to Eq. (6), the neutrino emissivity in the dUrca processes for both electrons and muons are shown in Fig. 2. It is found that the trend of the three curves is similar. The rise of every curve at low densities indicates the beginning of the dUrca process for the muons. However, the density ranges that the dUrca processes for both electrons and muons are allowed differ, which is also shown in Table 2. From Fig. 2 and Table 2, it is found that the critical density of the dUrca process for electrons or muons in the NL-SH set is the lowest, whereas that in the GPS250 set is the highest. The reason for this is that the Fermi momenta of protons and leptons in the NL-SH set increase much more rapidly than those in the GPS250 set. In the high density range where the dUrca processes of both electrons and muons are allowed, from Fig. 2 it is obviously seen that the three parameter sets lead to the disparity of the magnitudes of the neutrino emissivity. The values in the GPS250 set (dashed line) are the largest, the GM1 set (solid line) values are in the middle, and the smallest are in the NL-SH set (dotted line). The reason for this lies in Eq. (6), which indicates that the neutrino emissivity I mainly depends on the effective mass of nucleons and the chemical potentials of leptons. The results show that between the three parameter sets, the chemical potentials of leptons are similar, but the value in the NL-SH set is somewhat larger (see Table 3). However, the situation in the effective mass of nucleons $m^*_{\rm i}$ is reversed. From Eq. (7), we know that the effective mass of nucleons $m^*_{\rm i}$ is determined by the Fermi momenta of nucleons and the σ field. Although

the σ field becomes stronger with the density (see Fig. 1), which leads to the fall in $m_{\rm i}^*$, the Fermi momentum increases violently, and this effect is very obvious in the GPS250 set. Consequently, the GPS250 set leads to the maximum $m_{\rm i}^*$ in all the parameter sets. For example, we list the effective masses of nucleons and the chemical potentials of electrons at $4.46\rho_0$ in Table 3. It is seen that the effective masses of nucleons in the GPS250 set are more than those in the NL-SH set by almost a half, and they are obviously also higher than those in the GM1 set. This means that the magnitude of neutrino emissivity in the GPS250 set almost amounts to 3×10^{27} erg s^{-1} cm^{-3}, which is as large as two times that in the NL-SH set, and 1.5 times that in the GM1 set. Therefore, the effective masses of nucleons influence the neutrino emissivity elaborately. However, the cooling curves are not very sensitive to them, for example, in Ref. [19] the author set the effective mass $M^* = 0.7M$. Note that in Fig. 2 the neutrino emissivity in the GPS250 set in the nucleon-only matter increases with density. However, only at high densities does this phenomenon occur in the GM1 and NL-SH sets. Consequently, from Fig. 2 and Table 2, we can conclude that the GPS250 set, which leads to soft EoS, favors neutrino emission.

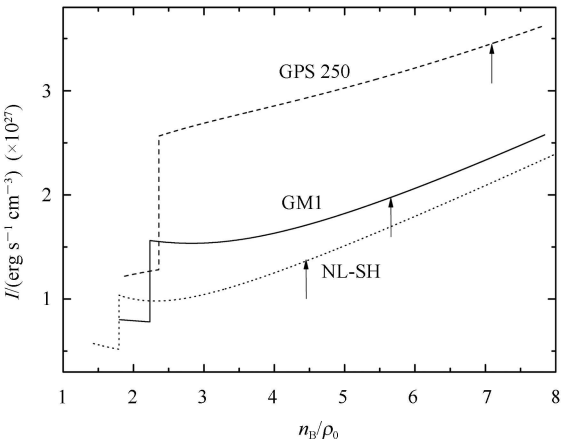

Fig. 2. The neutrino emissivity I of the dUrca processes for both electrons and muons as a function of density in nucleon-only matter in the GM1, GPS250 and NL-SH parameter sets, respectively. The arrowheads at every curve correspond to the maximum central densities, $u_{\rm cent}$.

Table 2. The density ranges that the dUrca processes for both electrons (dUrcae) and muons (dUrcaμ) are allowed in np matter.

	GM1	GPS250	NL-SH
$u_{\rm dUrcae}$	1.80–5.65	1.87–7.09	1.43–4.46
$u_{\rm dUrca\mu}$	2.23–5.65	2.36–7.09	1.79–4.46

For a neutron star with a fixed mass, we can give the neutrino luminosity L_ν by integrating the neutrino emissivity. The neutrino luminosities, L_ν, as a function of the mass of the neutron star in the GM1, GPS250 and NL-SH parameter sets are shown in Fig. 3. It is found that L_ν increases with the mass of the neutron star, especially when the dUrca processes for both electrons and muons occur, and the relation increases linearly. It is seen in Fig. 3 that the maximum neutrino luminosity $L_{\nu\rm max}$ in GPS250 has the largest value, whereas that in the NL-SH set is the smallest. The highest neutrino emissivity in the GPS250 set mainly accounts for this result. Note that the curve corresponding to the NL-SH set is not always the lowest in all the ranges of the masses of neutron stars. When the mass of the neutron star $M \leqslant 1.6M_\odot$, the neutrino luminosity in the NL-SH set is higher than that in the GM1 set. The reason for this is that the NL-SH set makes the critical density of the dUrca process lower (see Fig. 2 and Table 2), and in neutron stars with low masses the area where the dUrca process is allowed is wider in the NL-SH set than that in the GM1 set.

Table 3. The effective masses of neutrons and protons, $m_{\rm n}^*$ and $m_{\rm p}^*$, and the chemical potentials of electrons $\mu_{\rm e}$ at $4.46\rho_0$ in the GM1, GPS250 and NL-SH parameter sets in np matter.

	$m_{\rm n}^*/\mathrm{fm}^{-1}$	$m_{\rm p}^*/\mathrm{fm}^{-1}$	$\mu_{\rm e}/\mathrm{fm}^{-1}$
GM1	2.79122	2.13862	1.40978
GPS250	3.47849	2.96383	1.39868
NL-SH	2.52197	1.87293	1.42316

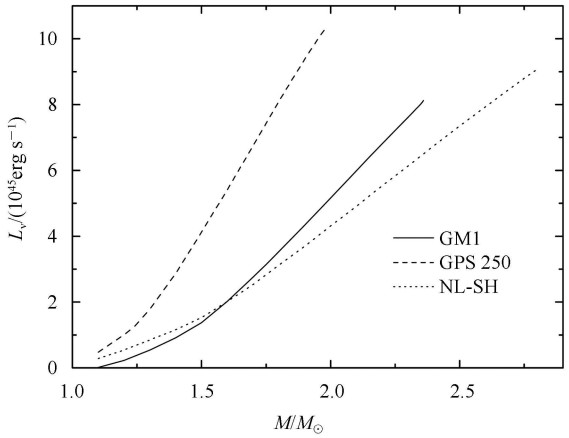

Fig. 3. The neutrino luminosity L_ν as a function of the mass of the neutron star in the GM1, GPS250 and NL-SH parameter sets in np matter.

Cooling curves, which can be obtained through Eq. (9), are shown in Fig. 4. It is found that the curves due to the various parameter sets are quite different. Curves corresponding to the GPS250 set are the lowest and those corresponding to the NL-SH set are the highest, which means that the neutron stars derived from the GPS250 parameter set cool quickly, but those in NL-SH cool slowly. The cooling rates of neutron stars in the

GM1 set are in the middle. It is seen that neutron stars in the GPS250 set need roughly 110 y to enable the temperature to fall to 4×10^8 K from 10^9 K, whereas those in the NL-SH set need about 360 y and those in the GM1 set 260 y. Therefore, neutron stars in the GPS250 set obviously cool faster than those in the NL-SH set, and the high neutrino luminosity and low specific heat of the neutron star are mainly responsible for this result. So we can conclude that in nucleon-only matter, the stiffer the EoS is due to the parameter set, the slower the corresponding neutron stars cool. It is also found from Fig. 4 that the more massive star cools faster in every parameter set.

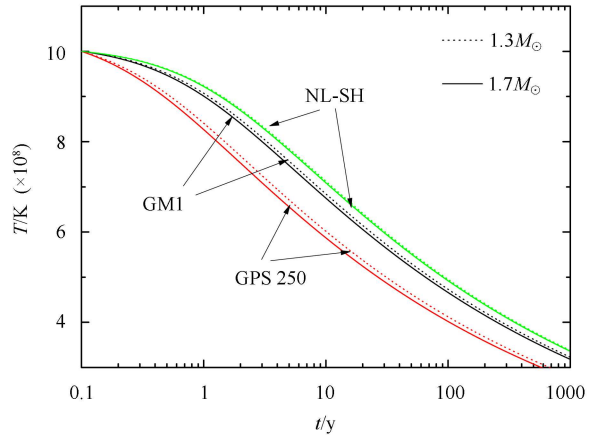

Fig. 4. Cooling curves of interior temperature versus time in the three parameter sets in np matter. Two masses of neutron stars are considered: $1.3M_\odot$ (dotted lines) and $1.7M_\odot$ (solid lines). The initial temperature and time are assumed to be 10^9 K and 0.1 y, respectively.

Considering the effects of the hyperon Λ, we list the results in Table 4 and Fig. 5. Here we only investigate how hyperons affect the dUrca process for nucleons, because although the direct Urca process with hyperons belongs to the enhanced cooling mechanism, the neutrino emissivity is about a 10^2–10^3 order lower than that of the dUrca process for nucleons. From Table 4 it is seen that in npΛ matter, the critical densities of the dUrca process with muons in the three parameter sets are all higher, respectively, compared with those in np matter (see Table 2). The presence of Λ is responsible for the changes. As we know, the appearance of hyperons makes the energy of the star lower, and consequently the Fermi momenta of nucleons and leptons fall, compared with the nucleon-only matter. This means that the condition of the dUrca process with muons (Eq. (8)) can only be satisfied at a higher density. However, compared with Table 2, it is found in Table 4 that the effect where the hyperon Λ postpones the occurrence of the dUrca process with muons is strongest in the GM1 set, weakest in the GPS250 set, and in the middle in the NL-SH set.

Table 4. The maximum mass $M_{\rm max}/M_\odot$, the corresponding central densities $u_{\rm cent}$ and the radii R of neutron stars in npΛ matter for the three parameter sets. The density ranges where the dUrca process for muons are allowed and the critical density of Λ hyperons are listed.

	GM1	GPS250	NL-SH
$M_{\rm max}/M_\odot$	2.088	1.772	2.466
R/km	11.287	10.720	12.617
$u_{\rm cent}$	6.62	7.81	5.33
$u_{\rm cr}(\Lambda)$	1.76	2.23	1.64
$u_{\rm dUrca\mu}$	2.39–6.62	2.38–7.81	1.86–5.33

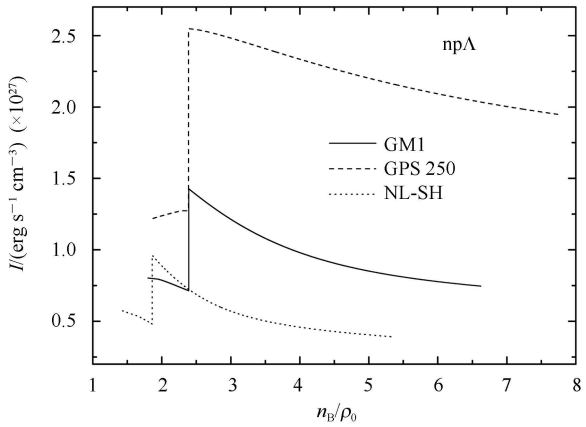

Fig. 5. Similar to Fig. 2, but for npΛ matter. The terminal point of every line corresponds to the central density of the maximum mass star.

Figure 5 shows the neutrino emissivity of the dUrca processes with both electrons and muons in npΛ matter. Compared with the results in the np matter (Fig. 2), it is found that the magnitude of neutrino emissivity in npΛ matter is obviously lower. It is seen that the maximum neutrino emissivity in Fig. 5 is about 2.7×10^{27} erg s^{-1} cm^{-3}, however that in Fig. 2 almost amounts to 3.5×10^{27} erg s^{-1} cm^{-3}. It is also seen that neutrino emissivity decreases with density in almost all the parameter sets in npΛ matter, except for a thin low density range in the GPS250 set. This indicates that the hyperon Λ reduces the neutrino emissivity. The reason for this is that the presence of Λ reduces the increasing rate of the Fermi momenta of nucleons and leptons. According to Eq. (8), the magnitude and trend of neutrino emissivity are consequently quite different in npΛ matter compared with np matter. However, the changes due to the presence of Λ in the GPS250 set are the smallest in all the parameter sets. Referring to the neutrino emissivity, from Fig. 9 in Ref. [20], we find similar results to ours, but Yin et al. considered more kinds of hyperons. In their Fig. 9, the neutrino emissivity due to the dUrca process in the highest density range increases with the radius r, but

the phenomenon is not obvious. The reason may be that in Ref. [20] the meson-hyperon coupling constants are set the same to nucleons, which makes the critical density of the hyperons lower, but the roles of the hyperons weaker.

5 Summary

In the framework of the RMFT and the related weak interaction theory we have studied the neutrino emission and cooling properties of neutron stars from the direct Urca process of nucleons in GM1, GPS250 and NL-SH nucleon coupling constant sets in nucleon-only and hyperonic matter. The results show that the potentials of mesons change with different parameter sets in the strong interaction. Consequently, the magnitude of the neutrino emissivity and the density ranges where dUrca processes are allowed are quite different between the three parameter sets. The GPS250 set leads to the maximum value of neutrino emissivity, however, the NL-SH set makes the critical density of the dUrca process the lowest. The highest neutrino luminosity is also derived from the GPS250 set. For stars $M>1.6M_{\odot}$, the neutrino luminosity is slightly higher in the GM1 set than in the NL-SH set in nucleon-only matter. The cooling curves of neutron stars in various parameter sets differ violently in nucleon-only matter. Stars in the GPS250 set cool very quickly, whereas those in the NL-SH set cool slowly, and the cooling rate of the former can be roughly three times larger than the latter. However, neutron stars in the GM1 set cool at a moderate pace. With the presence of the hyperon Λ, the critical density of the dUrca process with muons becomes higher, and the magnitude of neutrino emissivity becomes lower, compared with nucleon-only matter. These Λ effects are the strongest in the GM1 set and weakest in the GPS250 set. Therefore, we can conclude that nucleon parameter sets can have an obvious effect on cooling properties. The parameter set corresponding to softer EoS makes the neutron star cool faster. The hyperon Λ blocks neutron star cooling via the dUrca process for nucleons, and this effect differs in the various parameter sets.

References

1 Glendenning N K. Astrophys. J., 1985, **293**: 470–493
2 Kaplan D B, Nelson A E. Phys. Lett. B, 1986, **175**: 57–63
3 Nelson A E, Kaplan D B. Phys. Lett. B, 1987, **192**: 193–197
4 Banik S, Bandyopadhyay D. Phys. Rev. D, 2003, **67**: 123003-1–123003-10
5 Pal S, Bandyopadhyay D, Greiner W. Nucl. Phys. A, 2000, **674**: 553–577
6 DING W B, LIU G Z, ZHU M F et al. Chin. Phys. Lett., 2008, **25**: 458–461
7 Lattimer J M, Pethick C J, Prakash M et al. Phys. Rev. Lett., 1991, **66**: 2701
8 Kubis S, Kutschera M. Nucl. Phys. A, 2003, **720**: 189
9 Kubis S. Phys. Rev. C, 2006, **73**: 015805
10 Negreiros R, Schram S. Phys. Rev. D, 2012, **85**: 104019
11 Glendenning N K, Moszkowski S A. Phys. Rev. Lett., 1991, **67**: 2414
12 Furnstahl R J, Tang H B, Seort D B. Z. Phys. A, 1995, **52**: 1368
13 Lalazissis G A, Konig J, Ring P. Phys. Rev. C, 1997, **55**: 540
14 Reinhard P G. Z. Phys. A, 1998, **329**: 257
15 Leinson L B. Nucl. Phys. A, 2002, **707**: 543–560
16 Yakovlev D G, Kaminker A D, Gnedin O Y et al. Phys. Rep., 2001, **354**: 1
17 Boguta J, Bodmer A R. Nucl. Phys. A, 1977, **292**: 413
18 DING W B, LIU G Z, ZHU M F et al. Commun. Theor. Phys., 2010, **54**: 500–508
19 Leinson L B. Phys. Rev. C, 2011, **84**: 045501
20 YIN S Y et al. arXiv: 1112.1880